Ultrafast Charge Separation from the S_2 Excited State of Directly Linked Porphyrin−Imide Dyads: First Unequivocal Observation of the Whole Bell-Shaped Energy-Gap Law and Its Solvent Dependencies

Noboru Mataga,* Haik Chosrowjan, Seiji Taniguchi, and Yutaka Shibata†

Institute for Laser Technology, Utsubo-Hommachi 1-8-4, Nishi-ku, Osaka 550-0004, Japan

Naoya Yoshida and Atsuhiro Osuka*

Department of Chemistry, Graduate School of Science, Kyoto University, and CREST, Japan Science and Technology Corporation (JST), Kyoto 606-8502, Japan

Takeshi Kikuzawa and Tadashi Okada*

Department of Chemistry, Graduate School of Engineering Science, Osaka University, Toyonaka 560-8531, Japan

Received: June 28, 2002; In Final Form: October 11, 2002

Photoinduced charge separation (CS) due to electron transfer from the S_2 state of zinc porphyrin (ZP) to a directly linked imide (I) has been studied by means of femtosecond fluorescence up-conversion and femtosecond−picosecond transient absorption spectral measurements. S_2 fluorescence decay curves of ZP−I dyads in various solvents were all single-exponential, from which accurate rate constants for the CS reaction were obtained. The whole bell-shaped energy-gap law (EGL) has been confirmed unambiguously in polar solvents tetrahydrofurane, acetonitrile, and triacetin as the first example for CS, which can be reproduced on the basis of a nonadiabatic mechanism considering solvent reorganization and intrachromophore high-frequency vibrations (*hfm*) approximated by an averaged single mode. Mainly the top and inverted regions have been observed in nonpolar solvents cyclohexane and toluene. This result may be ascribed to the large decrease of the solvent reorganization energy in nonpolar solvents, which causes a large shift in the reaction coordinate for CS, making the S_2-state surface partially embedded in that of the CS state and transforming the EGL for the CS reaction into one that is somewhat analogous to that of the radiationless transition in the weak-coupling limit. The single-exponential fluorescence decay in 100 fs and the EGL with both normal and inverted regions observed in triacetin indicate strongly that very fast solvent relaxation should take place despite the very long τ_L of 125 ps at 20 °C (see the text). Thus, by using specifically designed ZP−I linked systems, we have directly demonstrated that both the intramolecular *hfm* and ultrafast solvent relaxation play very important roles in the ultrafast CS from the S_2 state and that we can regulate its EGL by controlling the nature of the solvent.

Introduction

The dynamics and mechanisms of photoinduced electron transfer (ET) in condensed media are the most important fundamental problems in chemistry and biology.[1−13] The photoinduced ET reactions are regulated by various factors including the magnitude of electronic interaction responsible for ET between the electron donor (D) and acceptor (A), the free-energy gap between the initial and final states of the ET process, interactions with the environment including solvation dynamics, and the intramolecular vibrations of solutes D and A coupled with the ET process facilitating it.[1−13]

Among many features, the energy-gap dependence of ET reactions is especially diagnostic in testing ET theories, and one puzzling aspect was the lack of unambiguous observation of the inverted region in the photoinduced charge-separation (CS) reactions despite extensive related studies.[6−9,12,13] In the case of the reaction between the excited fluorescer molecule and the electron-accepting or -donating quencher molecule for a diffusional encounter in polar solutions, the k_{CS} value for the favorable region of the energy gap $-\Delta G_{CS}$ is masked by the diffusion limit, as shown by the well-known work of Rehm and Weller[14] (stationary fluorescence-quenching measurements). "True" k_{CS} values higher than those given by Rehm and Weller were estimated by analyzing the transient effect in the fluorescence-quenching dynamics, which indicated, however, a very broad and rather flat k_{CS} versus $-\Delta G_{CS}$ relation showing no inverted region.[8,9,12,13] This result can be interpreted in terms of the distance distribution between the fluorescer and quencher for the CS process and the increase in the average distance with an increase in $-\Delta G_{CS}$. Namely, a large solvent reorganization energy λ_s (eq 4) is favorable to keeping the rate constant k_{CS} large for a larger energy gap $-\Delta G_{CS}$, and a large λ_s means a large D−A encounter distance. This distance-distribution effect makes the observation of the inverted region for the CS reaction

* Corresponding authors. Fax: 81-66-443-6313.

† Present affiliation: Department of Materials Science, Graduate School of Science, Nagoya University, Furocho, Chikusa-ku, Nagoya 464-8602, Japan.

10.1021/jp021522z CCC: $22.00
Published on Web 12/04/2002

very difficult.[6−9,12,13] Therefore, to circumvent the CS distance-distribution effect, many distance-fixed D−A molecules including porphyrin (D) and quinone or imide (A) have been prepared and subjected to ultrafast measurements.[1,4−8,12,15−19] Nevertheless, it has remained difficult to demonstrate the whole bell-shaped energy-gap dependence including a distinct inverted region for the photoinduced CS reaction so far.

This difficulty may be ascribed to an insufficient energy gap available for the photoinduced CS reaction from the S_1 state. In this respect, we have attempted to utilize a large energy gap for CS from the S_2 state of porphyrin toward a directly linked electron acceptor. Some porphyrin derivatives such as ZnDPP (Zn-5, 15-bis (3, 5-di-*tert*-butylphenyl)-porphyrin) and ZnTPP (Zn-tetraphenylporphyrin) show weak fluorescence of a relatively long lifetime (~2 ps) from the S_2 state in competition with internal conversion (IC) to the S_1 state, which is very favorable for the studies on the ultrafast reaction dynamics from the S_2 state using the femtosecond fluorescence up-conversion technique. Moreover, we have made femtosecond fluorescence dynamics measurements on these porphyrins and have elucidated the detailed mechanisms of their $S_2 \rightarrow S_1$ IC and succeeding ultrafast vibrational redistribution, giving the vibrational states mainly near the bottom of S_1 and also various nonrelaxed vibrational states emitting very weak hot fluorescence.[38] In the present study of the CS process from the S_2 state, we have used a series of supramolecular systems where ZnDPP (abbreviated hereafter as ZP) is directly linked at the meso position to the acceptor (a series of imide compounds, abbreviated as I) so that the D−A electronic interaction is strong enough to realize the CS process to the extent that is sufficient to detect in competition with the $S_2 \rightarrow S_1$ IC.

However, the solvent relaxation dynamics significantly affects the ET process,[10,11] and we expected the ET process to be limited by the solvent relaxation time τ_L when the ET dynamics becomes very fast. However, especially in the case of the excited-state ET reaction, the coupling with intramolecular high-frequency modes (*hfm*) of the solute molecules appears to facilitate the reaction, leading to a rate considerably larger than τ_L^{-1}.[10,11,16−24] Such an effect of the coupling with the intramolecular *hfm* was indicated to be especially large in the case of the ET reaction in the barrierless and inverted regions.[10,11,20−24] Moreover, it has become clear that ultrafast solvent relaxation in the 10−100 fs regime taking place in a much shorter time than τ_L can produce an ultrafast dynamics Stokes shift of the fluorescence and accelerate the photoinduced ET in polar solvents such as acetonitrile, alcohols, water, et cetera.[25−29] Therefore, both the coupling of the ET process with the intramolecular *hfm* and the ultrafast solvent relaxation ($\gg\tau_L^{-1}$) in some polar solvents seem to be capable of inducing ultrafast CS reactions in the excited electronic state.

In this work, we have made comprehensive investigations into the most fundamental aspects of photoinduced ET phenomena in the condensed phase, which still seem to need further elucidation, by utilizing the donor−acceptor directly linked ZP−I systems specially designed for such a purpose. Namely, we have made extensive examinations of the photoinduced CS processes from the S_2 state of a series of ZP−I systems to elucidate the following problems: (a) unequivocal observation of the whole bell-shaped energy-gap law (EGL) including a distinct inverted region, (b) isomorphism[10,11,22,23] or the difference between the EGL of photoinduced CS from S_2 for the ZP−I systems and that of the IC in the weak-coupling limit, (c) modification of the nature of the EGL for the CS from the S_2 state of ZP−I by a change in the nature of the solvent, (d) effect of the polar solvent relaxations on the very fast photoinduced CS dynamics of ZP−I in the S_2 state, including the problem of its dependence on the solvent τ_L or the much faster solvent relaxation ($\gg\tau_L^{-1}$) as well as on intramolecular *hfm*, and (e) effects of the temperature and excitation wavelength or the excess vibrational energy on the ultrafast CS from the S_2 state of ZP−I and its relation to the EGL of the CS reaction.[10,11,22,23]

In addition, concerning the above investigations using the ZP−I systems, we should note here that not only the above-discussed mechanisms of the photoinduced CS but also other more or less specific mechanisms are working in the actual photoinduced ET phenomena in the condensed phase. Some important examples of previous investigations in relation to the above-described problems for the photoinduced CS reactions of ZP−I systems are briefly summarized below.

We have investigated the dynamics and mechanisms of photoinduced ET in solutions with femtosecond−picosecond laser spectroscopy not only in the case of the inter- and intramolecular ET by weak donor−acceptor interactions in polar solutions[1,8,9,12,30] but also those by strong interactions where the reaction proceeds by excited CT (charge transfer) complex or exciplex (EX) formations and subsequent complete CS into ion radical pairs (IP).[1,8,9,12,30−33] The photoinduced ET in the case of strong donor−acceptor interactions can also take place in the excited hydrogen-bonding complexes between such aromatic proton donor and acceptor as aminopyrene−pyridine and pyrenol−pyridine in nonpolar solvents, where the photoinduced ET is facilitated by a coupled-proton shift or a transfer in the hydrogen bond according to our femtosecond−picosecond laser spectroscopy studies.[8,12,34]

We have also elucidated the fact that the EGL for the radiationless CR (charge recombination) deactivation of those IPs with compact structures (compact IP, CIP) formed by excitation of the ground-state CT complex is quite different from the Marcus parabola and is expressed by the exponential decrease of the CR rate constant with an increase in the free-energy gap.[8,12,33] This EGL is isomorphous with the EGL of the intramolecular radiationless transition in the weak-coupling limit.[8,12,33,36,37] Moreover, only a small solvent polarity effect on the exponential EGL of CIP has been observed,[33] and exactly the same EGL has been observed for the CIP adsorbed on porous glass without solvent.[35] These results indicate strongly that the intramolecular *hfm* plays a predominant role and that polar-solvent reorganization is not important in the CR of the CIP. Furthermore, the activation energy for CR measured in the adsorbed state was very small.[35] We present detailed comparative discussions of the EGL of CIP and the EGL of the photoinduced CS reaction of the ZP−I systems in various solvents of different polarities in Results and Discussion.

Experimental Section

ZP−I samples were prepared by the condensation of a meso-aminated porphyrin with appropriate anhydrides or by meso substitution via the one-electron oxidation of a 5,15-diaryl zinc (II) porphyrin with an amide anion. Synthetic details will be reported elsewhere.[39] X-ray crystallography was performed on a RIGAKU-RAXIS imaging plate system. The one-electron oxidation (E_{ox}) and reduction (E_{red}) potentials (vs ferrocene/ferrocenium) of ZP−I samples were measured in DMF (*N*,*N*-dimethylformamide) by the cyclic voltammetry method and the differential pulse voltammetry method on a ALS electrochemical analyzer model 660 with reference electrode $Ag/AgClO_4$, working electrode Pt, counter electrode Pt, and supporting

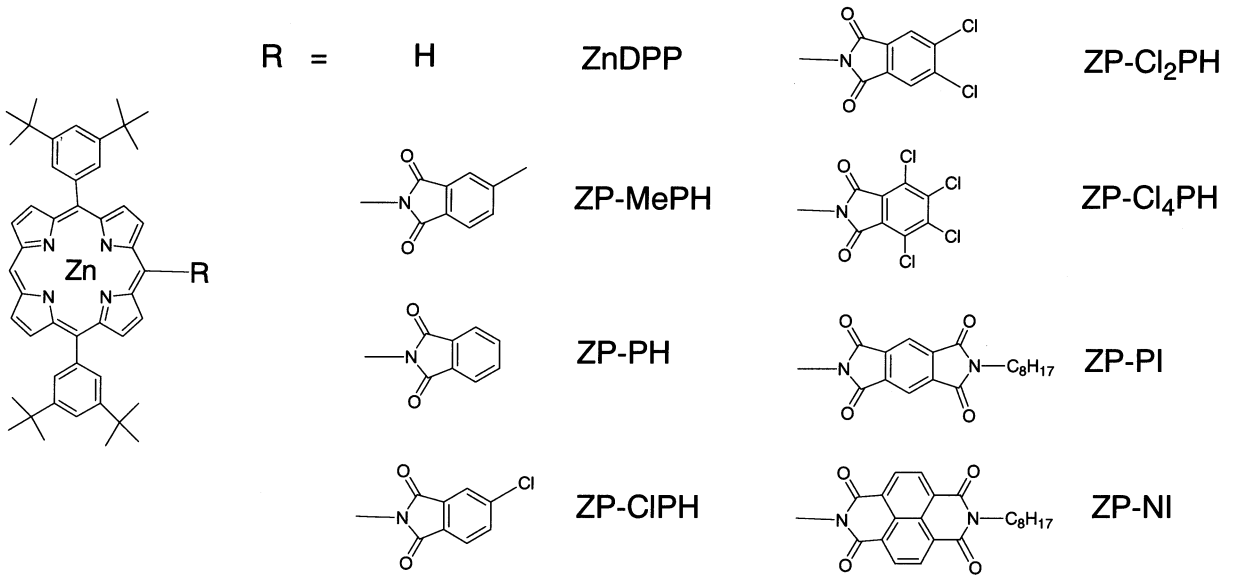

Figure 1. Structural formulas of the ZnDPP (ZP) and ZP−I dyads.

electrolyte/solvent Bu_4NBF_4/DMF 0.1 M. The energy of the ion-pair state, ZP^+-I^-, in DMF was obtained simply by ($E_{ox} - E_{red}$). Since the electrochemical measurements in less polar solvents such as THF were not very reproducible, we used the redox potentials in DMF for the estimation of the energy level of the ion-pair states as described in the text.

The measurements of the fluorescence decay dynamics were made on a fluorescence up-conversion apparatus similar to that described elsewhere,[38] but the fwhm of the instrumental response was improved to 110 fs. Transient absorption spectra of the $ZP^*(S_2)-I$ and ZP^+-I^- states of several ZP−I dyads were taken with the femtosecond−picosecond laser photolysis apparatus described elsewhere.[40]

All of the solvents used in this work (acetonitrile (ACN), triacetin (GTA), tetrahydrofurane (THF), toluene (Tol), and cyclohexane (CH)) were spectro or GC grade. A sample solution in an optical cell with a 2-mm path length was stirred by using a micro magnetic stirring bar during the measurements. By comparison of the absorption spectra before and after the measurements, it has been confirmed that the photodecomposition of ZP−I systems is negligibly small during the measurements. For the measurements of temperature effects on fluorescence dynamics in THF and Tol solutions, an optical cell containing the sample solution was set in a quartz Dewar with optical flat windows, and the temperature was controlled with a cold nitrogen gas stream. The observed fluorescence rise and decay curves were deconvoluted with the instrumental response function. Steady-state absorption spectra were recorded on a SIMADZU UV-3100PC UV−vis−NIR scanning spectrophotometer.

Results and Discussion

ZP−I Dyads. Structural formulas of ZP−I dyads are shown in Figure 1. Several properties of ZP−I that are important in understanding the ET dynamics are described here. Figure 2 (see also Supporting Information 1) shows the X-ray crystal structure of ZP−PH in which the phthalimide acceptor is held nearly perpendicular to the porphyrin plane with a dihedral angle of 88°. Similar perpendicular structures have been also obtained for ZP−MePH and ZP−Cl_2PH by X-ray crystallography (Supporting Information 2 and 3). In the ^{1}H NMR spectra, the β protons adjacent to the acceptor moiety appear at nearly the same chemical shifts throughout the series, indicating the similar perpendicular conformation of the imide acceptor moiety with respect to the porphyrin plane.

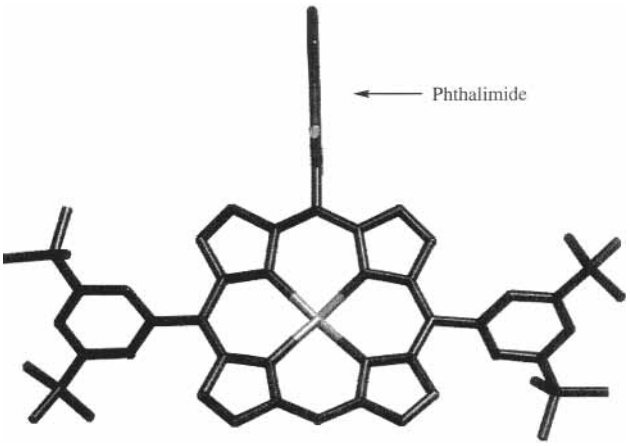

Figure 2. X-ray crystal structure of ZP−PH. The hydrogen atoms are omitted for clarity.

The absorption spectra of ZP−I dyads (Supporting Information 4) indicate that the excitation energy of the ZP S_2 state is practically the same (~2.9 eV) throughout the series, and there is no extra absorption band due to charge transfer (CT) as observed for the directly linked porphyrin−quinone systems[17,18] in the neighborhood of the S_1 transition. The peak position of the Soret band of the ZP−I dyads is only slightly red shifted from that of free ZP and is at almost the same position as that of 5,10,15-tris(3,5-di-*tert*-butylphenyl)-Zn-porphyrin ($ZnAr_3P$). These results indicate a rather weak D−A electronic interaction in ZP−I systems despite their directly linked structure. Such reduced electronic coupling in ZP−I may be ascribed to the nearly perpendicular conformation of the imide acceptor moiety as revealed by X-ray crystallography (Figure 2 and Supporting Information 1). We have further confirmed that the fluorescence decay time of $ZnAr_3P$ in the S_2 state (~2.33 ps) is practically the same as that of the reference ZP ($\tau_0 = 2.25$ ps). Therefore, one can safely evaluate the CS rate constant (k_{CS}) in the S_2 state from the relation $k_{CS} = \tau^{-1} - \tau_0^{-1}$.

Evaluation of the Free-Energy Gap ($-\Delta G_{CS}$) for the CS Reaction from the S_2 State of ZP−I Dyads. We have used

(a)

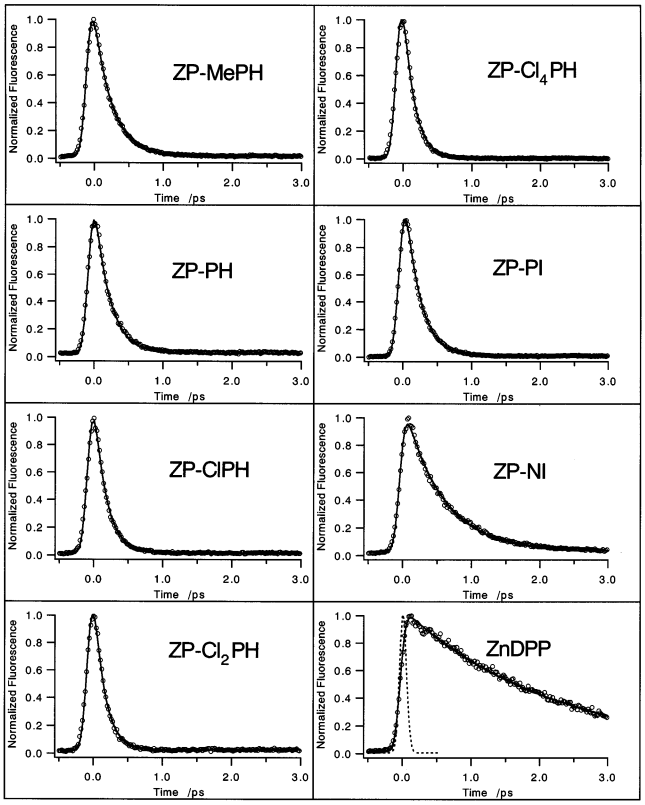
ZP-MePH
ZP-Cl4PH
ZP-PH
ZP-PI
ZP-ClPH
ZP-NI
ZP-Cl2PH
ZnDPP
Normalized Fluorescence
Time /ps

(b)

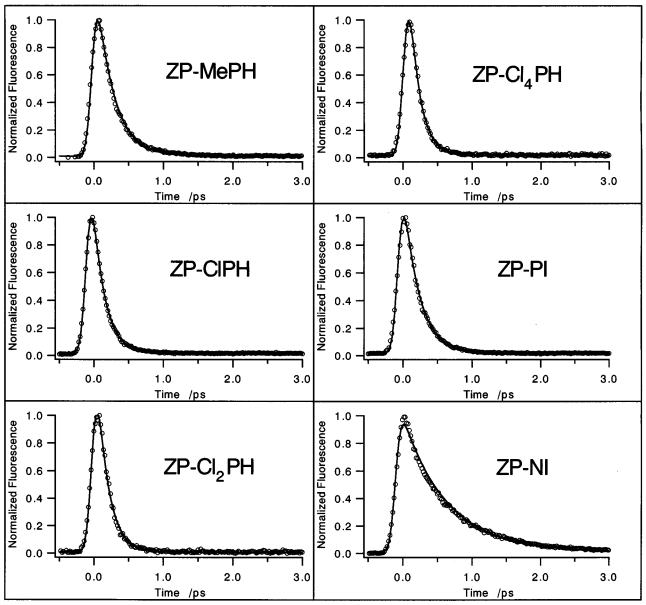
ZP-MePH
ZP-Cl4PH
ZP-ClPH
ZP-PI
ZP-Cl2PH
ZP-NI
Normalized Fluorescence
Time /ps

(c)

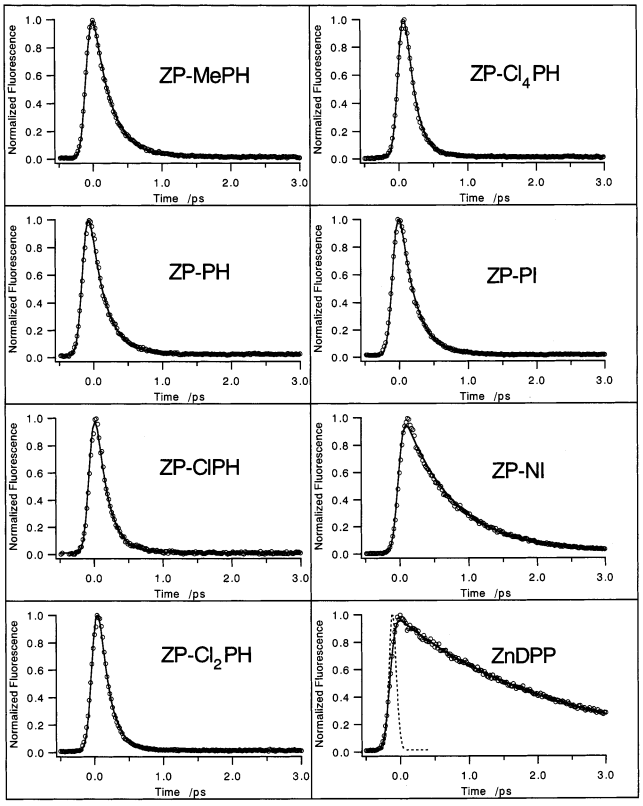
ZP-MePH
ZP-Cl4PH
ZP-PH
ZP-PI
ZP-ClPH
ZP-NI
ZP-Cl2PH
ZnDPP
Normalized Fluorescence
Time /ps

(d)

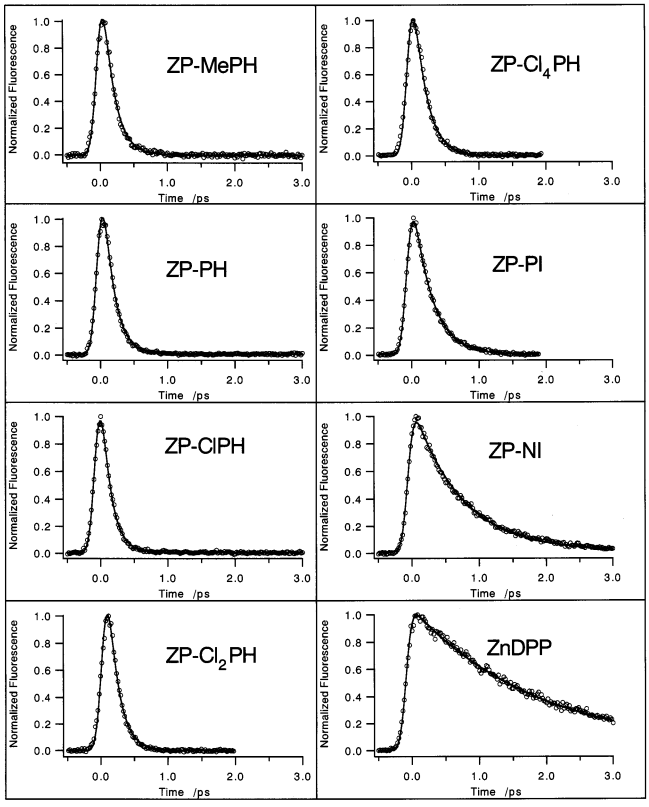
ZP-MePH
ZP-Cl4PH
ZP-PH
ZP-PI
ZP-ClPH
ZP-NI
ZP-Cl2PH
ZnDPP
Normalized Fluorescence
Time /ps

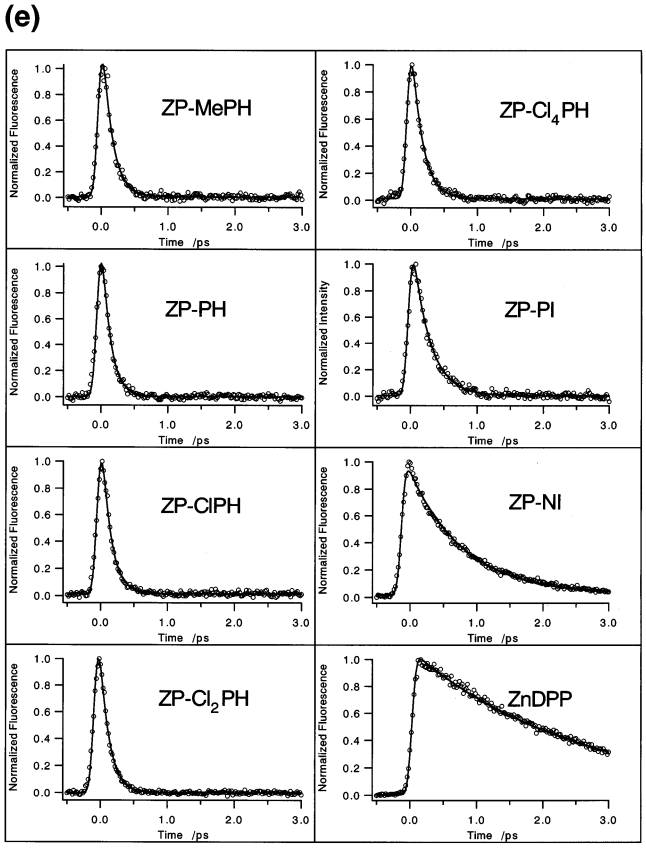

Figure 3 (cont'd). Fluorescence decay curves of ZP and ZP−I excited at 405 nm and monitored at 430 nm at 20 °C. Observed fluorescence rise and decay (○) and simulation with a single-exponential function taking into account the apparatus response (—). Solvents: (a) ACN, (b) GTA, (c) THF, (d) Tol, (e) CH.

the following equations based on the continuum approximation for solvents, where $\Delta E(S_2)$ is the energy gap between S_2 and S_0 of ZP, E_{ox} and E_{red} are, respectively, one-electron oxidation and reduction potentials of ZP and I in DMF, $-\Delta G_{CR}$ is the free-energy gap for the charge recombination (CR) of the intramolecular IP state ZP^+-I^- in the various solvents used here, and ΔG_S is the correction term that includes the effects of the solvent polarity and the Coulombic interaction energy between ZP^+ and I^-.

$$-\Delta G_{CS} = \Delta E(S_2) + \Delta G_{CR} \quad (1)$$

$$-\Delta G_{CR} = E_{ox} - E_{red} + \Delta G_S \quad (2)$$

$$\Delta G_S = e^2\left(\frac{1}{2r_D} + \frac{1}{2r_A}\right)\left(\frac{1}{\epsilon_s} - \frac{1}{\epsilon_r}\right) - \frac{e^2}{\epsilon_s r} \quad (3)$$

In eq 3, r is the center-to-center distance between ZP and I, r_D and r_A are the effective radii of the ZP^+ and I^- ions taken to be 5 and 3.5 Å (1,8/4,5-naphthalene tetracarboxylic diimide, pyromellitimide) or 3 Å (phthalimide derivatives), respectively, ϵ_r is the dielectric constant of the solvent in which E_{ox} and E_{red} have been determined (DMF), and ϵ_s is that of the solvent used for the fluorescence dynamics measurements.

In some cases of the photoinduced CS in the S_1 state of the D−A supramolecular systems, it is possible to estimate $-\Delta G_{CS}$ experimentally on the basis of the relationship $-\Delta G_{CS} = RT \ln(k_{CS}/k_{-CS})$ in which k_{-CS} is the rate constant of the reverse process of the photoinduced CS and is determined by measurements of the biphasic fluorescence dynamics of the S_1 state.[15,19b] With this $-\Delta G_{CS}$ value and the observed values of $\Delta E(S_2)$, E_{ox}, and E_{red}, one can determine ΔG_S experimentally and use it to estimate $-\Delta G_{CS}$ values for a series of D−A systems in a given solvent.[15,19b]

In the present systems, however, observation of the delayed S_2 fluorescence was not possible, probably because of the rapid deactivation of the CS state to lower states. Therefore, we must use eq 3 for the evaluation of ΔG_S. In the case of polar solvents THF and ACN, this is a reasonable approximation and has given satisfactory results in many cases according to previous studies.[1a,2,8,12,15] However, in the case of the less polar or almost nonpolar solvents, this approximation seems to give ΔG_S values that are too large.[15] Therefore, we have corrected the ΔG_S values in Tol and CH solutions, taking into consideration the experimentally obtained values in the S_1 state for the porphyrin−quinone[15] and zinc−porphyrin−free-base porphyrin[19b] dyad systems in benzene solution. Namely, the calculated ΔG_S values for Tol solution have been decreased by 0.35 eV to make them approximately equal to the experimentally determined values of those systems.[15,19b] For the CH solution, however, it is difficult to get an appropriate experimental value of ΔG_S. In the k_{CS} versus $-\Delta G_{CS}$ plot for CH solution in Figure 4, we have arbitrarily shifted the $-\Delta G_{CS}$ values by 0.3 eV to the positive side.

Similar circumstances also prevail in the case of the solvent reorganization energy λ_s given by eq 4 in the continuum approximation:

$$\lambda_s = e^2\left(\frac{1}{2r_D} + \frac{1}{2r_A} - \frac{1}{r}\right)\left(\frac{1}{\epsilon_\infty} - \frac{1}{\epsilon_s}\right) \quad (4)$$

The λ_s values for the photoinduced ET reaction of D−A dyads in benzene (Bz) and Tol solutions calculated with eq 4 are negligibly small because the optical dielectric constant ϵ_∞ is

very close to the static dielectric constant ϵ_s in these solvents. Nevertheless, λ_s values estimated to reproduce the observed k_{CS} versus $-\Delta G_{CS}$ relation in the S_1 state and the CR rate constant k_{CR} versus $-\Delta G_{CR}$ relation in the product IP state of porphyrin−quinone[15] and zinc−porphyrin−free-base porphyrin[19b] dyads in Bz and Tol solutions by means of the well-known eq 5 of Ulstrup and Jortner,[41] also taking into consideration the effect of the intramolecular *hfm*, are considerably larger (0.18 eV[15] and 0.35 eV[19b]) than the calculated values with eq 4.

$$k_{et} = (\pi/\hbar^2\lambda_s k_B T)^{1/2} V^2 \sum_n (e^{-S}(S^n/n!)) \exp\{-(\Delta G + \lambda_s + n\hbar\langle\omega\rangle)^2/4\lambda_s k_B T\} \quad (5)$$

where V is the D−A electronic-tunneling matrix element, $S = \lambda_v/\hbar\langle\omega\rangle$ is the electron−vibration coupling constant, and λ_v is the reorganization energy associated with the averaged angular frequency $\langle\omega\rangle$ of the *hfm*.

Large λ_s values in these almost nonpolar or only weakly polar solvents mean that there is a sizable solute−solvent polarization interaction in the course of the ET reaction. Actually, the large solvent reorganization energy[15] in Bz solution was interpreted by sophisticated theories[42] on the fundamental aspects of the solute−solvent interactions or by the interaction of the solute with the quadrupole moment of solvent Bz.[43] Such specific interactions between the excited solute and the "nondipolar" solvent are considered to lead to an anomalously large fluorescence Stokes shift by solvent reorganization, which was observed in the seminal works of fluorescence solvatochromism in 1955.[44,45]

Another problem concerning the evaluation of $-\Delta G_{CS}$ is that of the polar viscous solvent GTA. The observed ϵ_s value of GTA was reported many years ago to be 7.11 (at 20 °C),[46] which is slightly smaller than that of THF (∼8). However, the absorption spectral shift of a very polar solute ($E_T(30)$) in GTA suggests that its polarity is between that of THF and ACN.[47] Presumably, the $E_T(30)$ value may better represent the property of GTA as the microscopic environment surrounding the solute molecule. Moreover, as we discuss later in this article, the S_2 fluorescence decay dynamics of ZP−I in GTA is very similar to that in THF and ACN. Therefore, solvent reorganization associated with the CS process from the S_2 excited state in GTA seems to take place very rapidly (within the 10−100-fs regime) despite its very long τ_L (∼125 ps).[21] In view of these results, it may be reasonable to use a larger ϵ_s value than 7.11 for GTA in the present studies of the ultrafast CS dynamics from the S_2 excited state.

To estimate such a ϵ_s value for GTA, we tried the following procedures. In the previous study[48] of the electron transfer within the excited CT complex of TCNE (tetracyanoethylene)−HMB (hexamethylbenzene) in various solvents including THF, GTA and ACN, λ_s values were obtained on the basis of the fits to the CT absorption spectra. We have compared the value of λ_s(ZP−I) calculated from eq 4 with the experimental value of λ_s(CT complex) in the same solvent and have obtained the same value for the ratio $\chi = [\lambda_s(\text{ZP−I})/\lambda_s(\text{CT complex})] = 4.6$ in both THF and ACN. We have assumed the same value for χ in GTA and have obtained λ_s(ZP−I) ≈ 0.78 eV, from which ϵ_s(GTA) has been estimated to be 17.5 assuming that $\epsilon_\infty \approx 2$. With this ϵ_s value, the $-\Delta G_S$ and $-\Delta G_{CS}$ values for the ZP−I systems in GTA have been estimated.

Fluorescence Decay Dynamics of ZP−I Dyads. For all ZP−I dyads, very weak S_2 fluorescence emission was commonly observed in the same 420−450-nm wavelength region. Ultrafast S_2 fluorescence decays of ZP−I dyads and reference ZP in THF, ACN, GTA, Tol, and CH at 20 °C are shown in Figure 3. Although the measurements of the fluorescence decay dynamics of ZP−PH and ZP in GTA were not possible because of their poor solubility, the observed decay times of the other compounds in GTA were very close to those measured in THF and ACN. Therefore, we assumed the same τ_0 value for GTA solution as that of the THF solution. Most of the fluorescence decays of ZP−I were very rapid and were completed in 100-fs regime, and it is remarkable that all of the decays can be reproduced satisfactorily by a single-exponential function despite the wide range in solvent polarities, viscosities, and available energy gaps associated with CS.

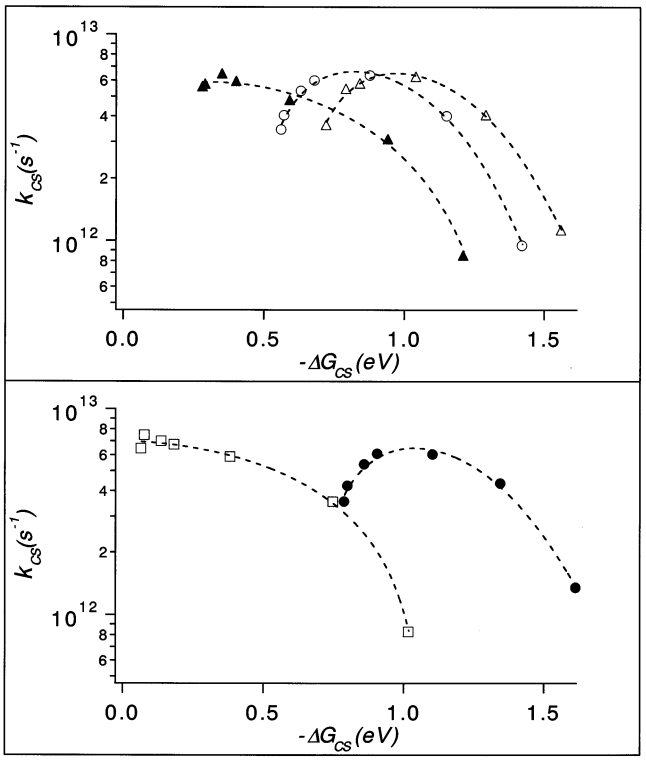

Figure 4. Observed k_{CS} vs $-\Delta G_{CS}$ relations in various solvents. The dotted lines are shown to guide the eye. Solvents: CH (□), Tol (▲), THF (○), GTA (△), and ACN (●). $-\Delta G_{CS}$ values in GTA were evaluated with ϵ_s(GTA) ≈ 17.5

In the present study, the solvent relaxation times τ_L are considerably different from each other (i.e., 0.1 ps (ACN), 0.5 ps (THF), and 125 ps (GTA) at ca. 20 °C[20,21,49]) where the τ_L of viscous GTA is especially large. In rapid ET reactions with time constants of ca. 0.1−1 ps, the solvent relaxation often poses a rate-determining step. Nevertheless, the fluorescence decay times in GTA are very close to those observed in ACN and THF, and the fluorescence decay dynamics in GTA is unambiguously single-exponential without any indication of multiexponential or nonexponential decays due to the ET at various solvation states along the slow solvation coordinate, as indicated by the Sumi−Marcus-type models.[4,20,21,28,50]

Fluorescence decay curves in slightly polar Tol and nonpolar CH solutions are similar to those in polar solutions. However, as shown in Figure 4, the indication of the normal region was very slight in Tol and CH solutions, whereas both the normal and inverted regions can be clearly observed in polar solvents THF, GTA, and ACN.

The ultrafast nature of the CS reactions from the S_2 state of these ZP−I systems and especially the above results of the ultrafast fluorescence dynamics due to the CS reaction in viscous GTA with a long solvation time τ_L suggest the important role

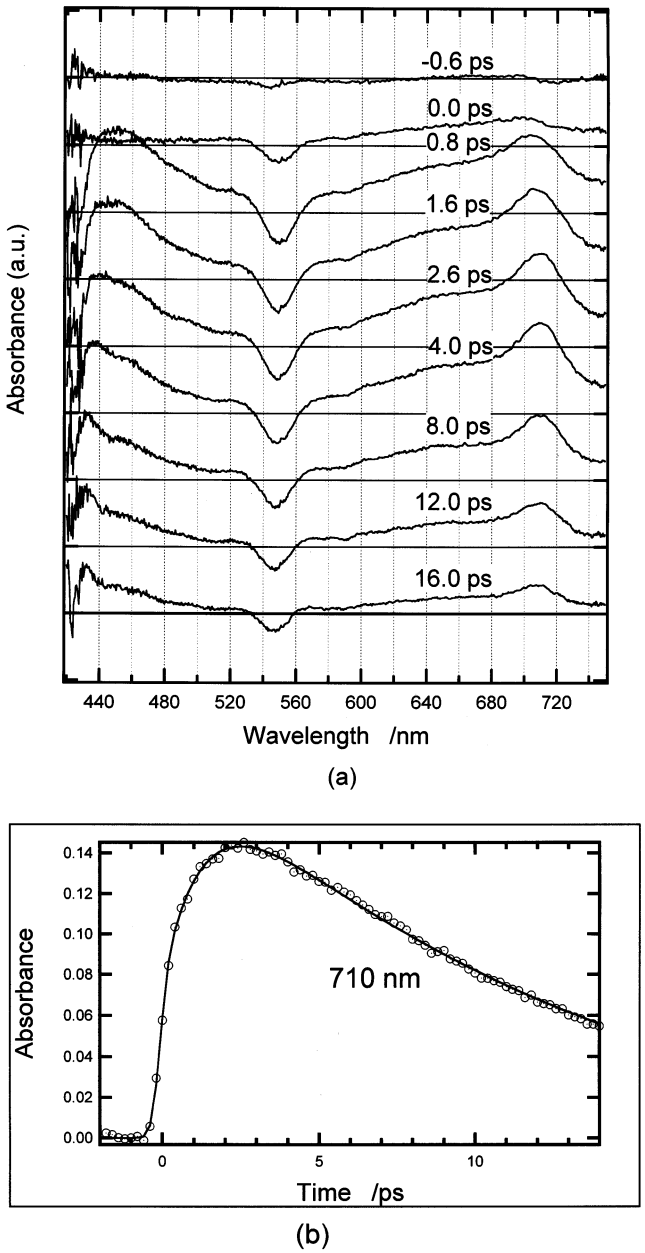

Figure 5. Time-resolved transient absorption spectra of ZP−PI in THF. (a) Time-resolved spectra in the 400−750-nm region exhibiting the characteristic PI^- band at 710 nm. (b) Absorbance rise and decay curve at 710 nm.

of coupling in the CS process with intramolecular *hfm*, which facilitates the reaction.[10,11,20−22] However, as discussed later in this article, one cannot simply ascribe the mechanism of the ultrafast CS in GTA only to the coupling with the intramolecular *hfm*.

Time-Resolved Transient Absorption Spectral Measurements. To confirm that the observed ultrafast fluorescence decay of ZP−I systems in the 100-fs regime is truly due to the ultrafast CS reaction from the S_2 state, we have examined the time-resolved transient absorption spectra of several ZP−I systems with the femtosecond−picosecond laser-photolysis apparatus.[40] A typical example of the time-resolved spectra of ZP−PI in THF solution is shown in Figure 5a, which shows the characteristic band due to the PI^- ion of the ion-pair state at 710 nm and bleaching at 550 nm immediately after S_2 excitation, providing firm evidence for the occurrence of CS. The time-dependent absorbance rise and decay curve at 710 nm is indicated in Figure 5b.

The transient absorption band of PI^- around 710 nm showed an ultrafast rise due to CS within ca. 200 fs (with a rate constant of $\sim 5 \times 10^{12} s^{-1}$). Immediately after the rise, the absorption band of PI^- was considerably broad and became sharpened and red-shifted within ca. 1 ps, producing an additional slower-rise component with an apparent rate constant of $\sim 1.0 \times 10^{12}$ s^{-1}, and the absorbance decayed with a rate constant of $\sim 7.0 \times 10^{10}$ s^{-1}. These spectral changes may be ascribed to the following processes. The ultrafast CS from the S_2 state produces the ZP^+-PI^- state with a large excess vibrational energy, which undergoes ultrafast vibrational redistribution, leading to the relaxed ZP^+-PI^- state exhibiting slightly sharpened and red-shifted spectra. The vibrationally relaxed ZP^+-PI^- state undergoes charge recombination decay to the ground state. The absorption band of PI^- in the relaxed ion-pair state is still broader than that of electrochemically generated PI^-.[51] This may be ascribed to a positive charge of ZP^+ proximate to PI^-. Thus, the faster rise at 710 nm with a rate constant of 5.0×10^{12} s^{-1} should correspond to the CS reaction from the S_2 state immediately after excitation (i.e., $k_{CS} = 5.0 \times 10^{12}$ s^{-1}). By means of similar analyses of transient absorption spectra, k_{CS} values for ZP−NI and ZP−MePH were estimated to be 9.5×10^{11} s^{-1} and 3.5×10^{12} s^{-1}, respectively. These k_{CS} values agree satisfactorily with those obtained by fluorescence up-conversion studies, as shown later.

Dependencies of the k_{CS} Values on the Excess Vibrational Energies in the Initial State and on the Temperature. We have examined the effect of the excess vibrational energy in the initial state (S_2) upon the ET dynamics of ZP−I systems. We have measured fluorescence decay dynamics both by excitation at 405 nm near the blue edge and at 425 nm near the red edge of the Soret band and have compared the obtained k_{CS} values. We have examined both THF and Tol solutions. In both solutions, the k_{CS} value obtained by blue-edge excitation was rather close to that obtained by red-edge excitation, which seems to be in agreement with the results of previous theoretical studies predicting a weak excess vibrational-energy dependence of photoinduced ET reactions[10,11] in the activationless (top) and inverted regions. Although the EGL of the CS reaction from the S_2 state of ZP−I systems shows the top and inverted regions with a slight indication of the normal region in Tol, the EGL in THF solution shows the distinct normal region, as indicated in Figure 4. Nevertheless, this normal region is rather close to the top region, and the activation barrier for the ET may be small, leading to the rather small effect of the excess vibrational energy. Another possibility for the small effect of the excess vibrational energy on the observed k_{CS} might be the ultrafast vibrational redistribution following the excitation to the hot S_2 state leading to the vibrational state near the bottom of S_2, from which the ET takes place in the case of the normal region in THF.

We have also examined the temperature dependencies of k_{CS} in THF solutions for ZP−MePH in the normal region, ZP−Cl_4PH in the top region, and ZP−NI in the inverted region by lowering the temperature from 20 to −80 °C, where the solvent remains in liquid phase. We have also examined the temperature dependence of k_{CS} for ZP−MePH in Tol solution, where the EGL of the CS reaction shows only a slight indication of the normal region. The results of these investigations have indicated that the effects of temperature lowering on the k_{CS} are not significant, which seems to originate from the same mechanism[10,11] as the weak dependence of k_{CS} on the excess vibrational energy in the initial state of the ET reaction, as described above.

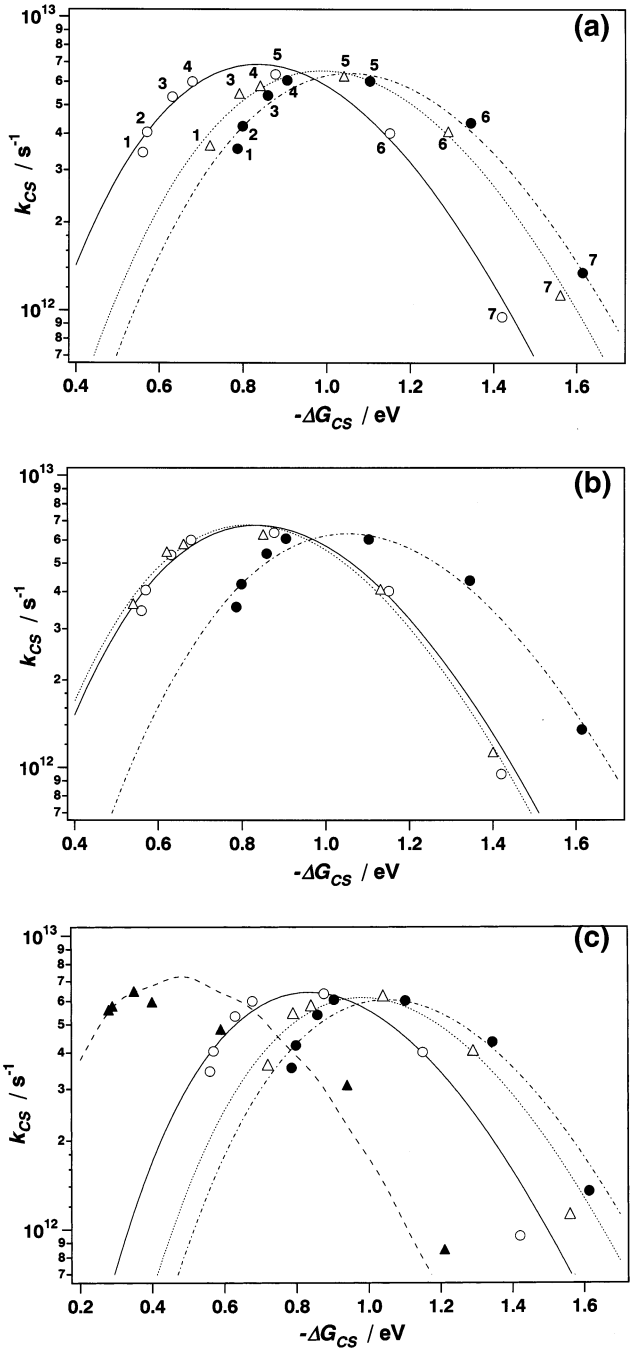

Figure 6. Energy-gap dependencies of k_{CS} and simulations with eq 5 at 20 °C (lines). Numerical values of parameters used in the simulation are shown in Table 1. Solvents: Tol (▲), THF (○), GTA (△), and ACN (●). Numbers of ZP−I: (**1**) ZP−MePH, (**2**) ZP−PH, (**3**) ZP−ClPH, (**4**) ZP−Cl_2PH, (**5**) ZP−Cl_4PH, (**6**) ZP−PI, and (**7**) ZP−NI. $-\Delta G_{CS}$ values in GTA were evaluated with ϵ_s(GTA) ≈ 17.5 (a, c) and ϵ_s(GTA) ≈ 7.1 (b).

Nevertheless, the k_{CS} value of ZP−NI is practically unchanged by the temperature lowering from 20 to −80 °C, whereas the k_{CS} values of the other systems, ZP−MePH and ZP−Cl_4PH, showed a small decrease from the temperature lowering. Since the CS reaction from the S_2 state of ZP−NI is deep in the inverted regime of the EGL, the potential energy surface of the S_2 state may be considerably embedded in that of the CS state, where the CS might take place predominantly coupled with the intramolecular *hfm* and might not be affected by the temperature change from 20 to −80 °C.

TABLE 1: Parameter Values in the Global Fitting with Equation 5 Corresponding to Figure 6a−c

(a) $-\Delta G_{CS}$ Values in GTA Evaluated with ϵ_s(GTA) ≈ 17.5

solvent	V/eV	λ_v/eV	λ_s/eV	$\hbar\langle\omega\rangle$/eV
THF	0.022	0.33	0.56	0.15
GTA	0.022	0.33	0.70	0.15
ACN	0.022	0.33	0.77	0.15

(b) $-\Delta G_{CS}$ Values in GTA Evaluated with ϵ_s(GTA) ≈ 7.1

solvent	V/eV	λ_v/eV	λ_s/eV	$\hbar\langle\omega\rangle$/eV
THF	0.022	0.36	0.52	0.15
GTA	0.022	0.36	0.50	0.15
ACN	0.022	0.36	0.73	0.15

(c) $-\Delta G_{CS}$ Values in GTA Evaluated with ϵ_s(GTA) ≈ 17.5

solvent	V/eV	λ_v/eV	λ_s/eV	$\hbar\langle\omega\rangle$/eV
Tol	0.023	0.40	0.15	0.17
THF	0.023	0.40	0.50	0.17
GTA	0.023	0.40	0.64	0.17
ACN	0.023	0.40	0.70	0.17

k_{CS} Versus $-\Delta G_{CS}$ Relations in Solutions of Different Polarities. In Figure 4, the obtained k_{CS} values of ZP−I compounds are plotted against $-\Delta G_{CS}$. Because the empirical method for the estimation of $-\Delta G_{CS}$ values is not possible in the present case, the absolute values of $-\Delta G_{CS}$ used here were corrected on the basis of the empirical values obtained for the CS in the S_1 state of the similar porphyrin−acceptor systems.[15,19] The relative values of $-\Delta G_{CS}$ corresponding to different ZP−I systems in the same solvent may be given reasonably well. The relative shift of the $-\Delta G_{CS}$ values from one solvent to another depending on the solvent polarity may also be given reasonably well for Tol, THF, and ACN but may be less reliable for CH. The estimation of the $-\Delta G_{CS}$ values for GTA seems to be a little complex. In Figure 4, the $-\Delta G_{CS}$ values for the GTA solvent were calculated by assuming that $\epsilon_s \approx 17.5$, which was estimated by the procedure described in Evaluation of the Free-Energy Gap ($-\Delta G_{CS}$). If we evaluate $-\Delta G_{CS}$ by using $\epsilon_s \approx 7.11$,[46] then the k_{CS} versus $-\Delta G_{CS}$ relation in GTA becomes very close to that of THF solution (as shown in Figure 6b). In any case, the inverted region in the EGL for the photoinduced CS reaction of the distance-fixed donor−acceptor dyads has been unequivocally observed for the first time in this work.

We have tried to reproduce the present results with eq 5, as shown in Figure 6 and Table 1. In this simulation, we first examined the observed results in polar solvents THF, GTA, and ACN. We have assumed that the values of parameters $\hbar\langle\omega\rangle$, λ_v, and V do not depend on the solvent because they are quantities proper to the solute molecule. Therefore, we have allowed these parameters to vary but under the condition that each of them has the same value in the three different solvents. The residual parameter λ_s was allowed to vary. The temperature was fixed at 20 °C, at which the measurements have been made. The lines in Figure 6a are the results of this global fitting procedure. The observed k_{CS} versus $-\Delta G_{CS}$ relations in polar solvents THF, GTA, and ACN can be reasonably well reproduced by the simulated curves. The parameter values summarized in Table 1a and b are close to those obtained in the previous simulations of photoinduced ET reactions of porphyrin−acceptor supramolecular systems[12,15,16,19] in polar solvents such as THF and ACN, except that V is a little larger because of the stronger D−A electronic interaction owing to the direct bonding without a spacer. In Figure 6a and Table 1a, $-\Delta G_{CS}$ for the GTA solvent was estimated, assuming the ϵ_s value to be 17.5. We have also examined the energy-gap dependencies

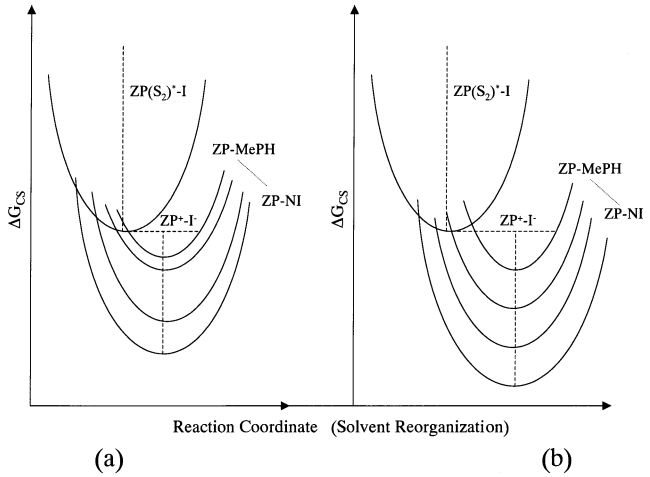

Figure 7. Schematic diagrams for the crossing between free-energy surfaces for $ZP(S_2)^*-I$ and ZP^+-I^- states. (a) In nonpolar or only slightly polar solvents (CH and Tol). (b) In polar solvents (THF, GTA, and ACN). These are drastically simplified 1D reaction-coordinate diagrams. Nevertheless, they show thatfor the results in Figure 4 only a slight indication of the normal region in addition to the top and inverted regions is observed in nonpolar solvents, whereas the whole normal, top, and inverted regions are detectable in polar solvents.

of k_{CS} in these polar solvents, assuming the ϵ_s of GTA to be 7.11. Results of the latter simulations are indicated in Figure 6b and Table 1b.

It is well known that, for the electron-transfer reaction in polar solvents, the solvent reorganization in the course of transfer plays the important role of the reaction coordinate and gives the activation free energy $(\lambda_s + \Delta G)^2/4\lambda_s$ according to the classical Marcus equation.[2] The fast relaxation of a polar solvent compared with the microscopic ET rate is responsible for the existence of a small activation barrier in the photoinduced CS reaction of the present dyad systems, which gives the normal region in the EGL of k_{CS} for the series ZP−MePH, ZP−PH, ZP−ClPH, ZP−Cl_2PH in THF, GTA, and ACN (Figures 4, 6, and 7b). However, in nonpolar or only slightly polar solvents such as CH and Tol, one can recognize only a slight indication of the normal-region-type EGL as shown in Figure 4. The reason for this may be ascribed to the much smaller solvent reorganization energies compared with those of the polar solvents as shown schematically in Figure 7a, which indicates that the EGL for these dyads in less polar or nonpolar solvents becomes somewhat similar to that of the intramolecular radiationless transition in the weak-coupling limit.[11,12,22,35−37] We have tried to extend our simulation of the observed k_{CS} versus $-\Delta G_{CS}$ relation with eq 5 to the Tol solution. In this case, we have again assumed that the parameters $\hbar\langle\omega\rangle$, λ_v, and V do not depend on the solvent. The lines in Figure 6c show the results of the global fitting, and the estimated parameters are summarized in Table 1c.

In Figure 6c, the observed results in polar solvents THF, GTA, and ACN are reasonably well reproduced by the simulation with eq 5. However, the results of the simulation for theTol solution are not satisfactory. This means that the EGL underlying the observed k_{CS} versus $-\Delta G_{CS}$ relation in Tol andCH solutions is a little different from that in the polar solvents. Namely, the energy-gap law assuming the single averaged *hfm* coupled with the electron-transfer process may be improper for the present results in nonpolar solvents.[11,22,23]

As discussed in previous sections, the energy-gap law for the k_{CS} versus $-\Delta G_{CS}$ relations of the present ZP−I systems in nonpolar solvents becomes somewhat similar to that of the intramolecular IC in the weak-coupling limit,[11,35,36] which shows the exponential energy-gap dependence. In such case, the energy-gap law cannot be described by eq 5 with a single *hfm* approximation; a multimode approximation seems necessary.[11,22,23] Our present studies on the ultrafast photoinduced CS from the S_2 state of ZP−I systems in several solvents of different polarities seem to suggest such a change in the EGL caused by changes in the solvent reorganization energy as well as the contribution of intramolecular *hfm*. In this respect, there is quite a different solvent effect on the EGL of the CR (charge recombination) reaction of the CIP (compact ion pair) produced by photoexcitation of the ground-state CT complex in solution[8,12,30,33] from that of the CS reaction of the S_2 state of ZP−I systems studied here.

In the case of the CIP formed by excitation of CT complexes between aromatic hydrocarbons and various electron acceptors such as tetracyanobenzene, tetracyanoethylene, phthalic anhydrides, et cetera, the EGL of the rate constant k_{CR} of the CR reaction of CIP can be reproduced satisfactorily by eq 6.[8,12,30,33]

$$k_{CR} = \alpha \exp(-\beta|\Delta G_{CR}|) \tag{6}$$

This simple equation for the exponential decrease of k_{CR} with an increase of the energy gap $-\Delta G_{CR}$ is isomorphous with the equation of the rate constant of the intramolecular radiationless transition in the weak-coupling limit.[36,37] On the basis of the previous theoretical treatment of the radiationless transition, it is possible to give an approximate equation for the energy-gap dependence of k_{CR} (eq 7).[36]

$$k_{CR} = C \exp[-(\{\gamma\}/\{\hbar\omega_M)|\Delta G_{CR}|\}] \tag{7}$$

$$\gamma = \ln(|\Delta G_{CR}|/S_M\hbar\omega_M) - 1 \tag{7a}$$

$$S_M = \sum_j S_j \tag{7b}$$

$$\omega_M = \sum_j \omega_j S_j / \sum_j S_j \tag{7c}$$

$$S_j = \frac{1}{2}(M_j\omega_j/\hbar)(\Delta Q_j)^2 \tag{7d}$$

where the factor C represents mainly the contribution from the electronic coupling term between the excited and ground states. The term $-(\gamma/\hbar\omega_M)|\Delta G_{CR}|$ arises from the energy release into acceptor modes in the CIP → ground-state transition. S_M and ω_M are average quantities for electron−vibrational coupling constants and angular frequencies of the quantum modes, respectively, where contributions from individual acceptor modes j are given by eqs 7b and 7c. The S_j is given by eq 7d as a function of the equilibrium displacements ΔQ_j, and M_j is the reduced mass for the vibration.

In general, the right-hand side of eq 6 should contain the term due to the solvent reorganization because both intramolecular modes and solvent modes are important. Nevertheless, it has been confirmed that the solvent polarity and solvent reorganization do not affect the observed $k_{CR} \approx -\Delta G_{CR}$ relations for the CIP in solution, and even for the CIP in the adsorbed state on porous glass in the absence of solvent, the same $k_{CR} \approx -\Delta G_{CR}$ relations as in strongly polar solutions are observed.[8,12,30,33,35] These results of the solvent effects upon the EGL for the k_{CR} of CIP are in marked contrast to the solvent effects upon the EGL for the k_{CS} of ZP−I systems in the S_2 state, as discussed above. Furthermore, not only in the case of the CR reaction of the CIP but also in the case of the CS reaction

from the S_1 state of cyclophone-bridged porphyrin−quinone systems the EGL does not seem to be affected by the change in solvent polarity.[16] Although the reason for the difference between ZP−I systems and CIP or cyclophane-bridged porphyrin−quinone systems is not very clear at the present stage of the investigation, the microscopic solvation structure of ZP−I may be somewhat different from that of CIP or cyclophane-bridged porphyrin−quinone system. Presumably, it may be difficult for solvent molecules to enter between molecular planes of CIP or those of cyclophane-bridged porphyrin and quinone. Contrary to these cases, more extensive solvation may be possible for the ZP−I systems, leading to a stronger solvation effect on the EGL of the photoinduced CS reaction.[11,12,22]

The existence of the normal region in the EGL of ZP−I systems in polar solvents indicates that the solvent relaxation is fast compared with the microscopic ET rate, and thermal equilibration prevails in these polar solvents where the barrier crossing by thermal activation takes place, resulting in the normal-region-type EGL and exponential decay of S_2 fluorescence. It should be emphasized here that the S_2 fluorescence decay dynamics of all ZP−I systems examined here in various solvents was definitely single-exponential in 100-fs regime and that normal-region-type energy-gap dependencies were unambiguously observed not only in ACN and THF but also in GTA, in addition to those in the inverted region. This means that, even in the viscous GTA with $\tau_L \approx 125$ ps at 20 °C, fast solvent relaxation can take place and thermal equilibration prevails in the solution of excited ZP−I surrounded by GTA solvent, and this system is undergoing single-exponential fluorescence decay in the 100-fs regime without showing any nonexponential or multiexponential fluorescence decay due to the long relaxation time τ_L of GTA, as suggested by Sumi−Marcus-type models.[50]

Concerning this problem, there was an investigation of the fast response of GTA in the solvation dynamics studied by using optical-heterodyne-detected Raman-induced Kerr-effect spectroscopy, which predicted that about 25% of the solvation dynamics will occur in the 100-fs regime.[52] Moreover, according to the results of our studies of the dynamic Stokes shift (DSS) measurements on coumarin 153 dye fluorescence in GTA, ultrafast DSS in 100 fs (20−30%) in addition to the main components with very long relaxation times have been clearly recognized.

Therefore, the ultrafast solvent response in 100 fs coupled with ultrafast photoinduced CS exists not only in such nonviscous polar solvent as ACN, THF, et cetera but also in such "slowly relaxing" viscous polar solvent as GTA, where the CS from the S_2 state of ZP−I is completed in the 100-fs regime, certainly owing to the coupling with both the ultrafast response component in the solvent relaxation dynamics and the intramolecular *hfm*. Thus, both the intramolecular *hfm* and the ultrafast solvent response play important roles at the same time in the photoinduced CS from the S_2 state of the ZP−I dyads.

Concluding Remarks

In the Introduction of this article concerning the dynamics and mechanisms of the ultrafast CS reaction from the S_2 state of the ZP−I dyads, we have indicated several important problems related to the present work. We believe that our studies described above have contributed significantly to the elucidation of these problems, as briefly remarked on below.

(1) The S_2 fluorescence decays in the 100-fs regime due to the CS reaction from the S_2 state of these dyads are all single-exponential, from which the exact rate constants of the photoinduced CS have been obtained, leading to the first unequivocal demonstration of the whole bell-shaped EGL including normal and inverted regions for the photoinduced CS reaction in polar solvents THF, GTA, and ACN.

(2) The photoinduced CS dynamics in the very viscous polar solvent GTA with a long τ_L (125 ps at 20 °C) does not show multiexponential or nonexponential decays as indicated by the Sumi−Marcus-type models. This means that not only the intramolecular *hfm* but also the ultrafast response component in the solvent relaxation dynamics in GTA plays a supremely important role in the CS reaction from the S_2 state of the dyads.

(3) Despite the bell-shaped energy-gap law observed for the dyads in polar solvents, only a slight indication of the normal region in addition to the top and inverted regions has been observed in nonpolar solvents, which may be interpreted on the basis of the simplified reaction-coordinate diagram, showing that the solvent reorganization energy plays an important role in the activation free energy, producing the normal region at the small energy gap for CS in polar solvents, whereas the solvent reorganization energy becomes very small in nonpolar solvents and the reaction-coordinate diagram may become somewhat similar to that of the intramolecular radiationless transition (internal conversion) in the weak-coupling limit. Therefore, the reproduction of the observed k_{CS} versus $-\Delta G_{CS}$ relation in nonpolar solvents by the simple applications of eq 5 becomes less satisfactory.

(4) We have examined the effect of the excess vibrational energy on the ultrafast CS from the S_2 state of ZP−I by investigating the effects of temperature and excitation wavelength on the k_{CS} values. Both effects were rather small, in accordance with previous theoretical calculations that predict a weak excess vibrational-energy dependence of photoinduced ET reactions in the activationless and inverted regions.[10,11] The observed effect of the temperature lowering from 20 to −80 °C on the k_{CS} of ZP−NI in THF solution was negligibly small. Since the CS from the S_2 state of ZP−NI is deep in the inverted region and the potential energy surface of the S_2 state may be considerably embedded in that of the CS state, the CS from the S_2 state can take place predominantly coupled with the intrachromophore *hfm* independent of such a temperature change.

The results of the present studies confirm that both intramolecular *hfm* and ultrafast solvent relaxation dynamics (10−100 fs) control the rate of the ultrafast CS from the S_2 state of the ZP−I dyads. Moreover, we could modify to some extent the nature of the EGL of the CS reaction from the S_2 of ZP−I dyads by controlling the solvent polarity. In relation to those results, we need to make more-extensive and more-quantitative studies concerning the effects of the solvent dynamics on the ultrafast CS reaction and the solvent effects on the EGL of the CS in the S_2 state of ZP−I dyads using various solvents of different natures, including the hydrogen-bonding solvents and polymer solid environments in addition to the typical polar and nonpolar solvents. Moreover, to reveal the whole aspect of reaction dynamics after S_2 excitation, such as the CS and competing $S_2 \rightarrow S_1$ IC followed by ultrafast vibrational redistribution and the CR (charge recombination) leading to lower states, et cetera, it is necessary to make accurate measurements of the S_1 fluorescence dynamics by S_2 excitation in addition to S_2 fluorescence dynamics. Furthermore, the effects of the increase in the strength of the ZP−acceptor electronic interaction on the photoinduced CS dynamics and its EGL may also be important problems to be elucidated.

These investigations are very important to the clarification of the fundamental aspects of the photoinduced electron-transfer

phenomena, and detailed studies are now going on in our laboratories, the results of which will be reported shortly.

Acknowledgment. This work was partially supported by a Grant-in-Aid (nos. 13640519 and 12440196) from the JSPS. N.Y. thanks the JSPS Research Fellowship for Young Scientists. We express our gratitude to the reviewer for his illuminating comments.

Supporting Information Available: Crystal data and structural refinement of ZP−PH, X-ray crystal structures of H_2P−MPH and ZP−Cl_2PH, and absorption spectra of ZP, ZP−I, and $ZnAr_3P$ in THF. This material is available free of charge via the Internet at http://pubs.acs.org.

References and Notes

(1) (a) Mataga, N.; Ottolenghi, M. In *Molecular Association*; Foster, R., Ed.; Academic Press: London, 1979; Vol. 2, p 1. (b) Mataga, N. *Pure Appl. Chem*. **1984**, *56*, 1255.

(2) Marcus, R. A.; Sutin, N. *Biochim. Biophys. Acta* **1985**, *811*, 265.

(3) Maroncelli, M.; McInnes, J.; Fleming, G. R. *Science (Washington, D.C.)* **1989**, *243*, 1674.

(4) Barbara, P. F.; Jarzeba, W. *Adv. Photochem*. **1990**, *15*, 1.

(5) Verhoeven, J. W. *Pure Appl. Chem*. **1990**, *62*, 1585.

(6) *Electron Transfer in Inorganic, Organic and Biological Systems;* Bolton, J. R., Mataga, N., McLendon, G., Eds.; Advances in Chemistry Series 228; American Chemical Society; Washington, DC, 1991.

(7) *Dynamics and Mechanisms of Photoinduced Electron Transfer and Related Phenomena*; Mataga, N., Okada, T., Masuhara, H., Eds.; Elsevier: Amsterdam, 1992.

(8) Mataga, N.; Miyasaka, H. *Prog. React. Kinet*. **1994**, *19*, 317.

(9) Kakitani, T.; Matsuda, N.; Yoshimori, A.; Mataga, N. *Prog. React. Kinet.* **1995**, *20*, 347.

(10) Bixon, M.; Jortner, J. *Chem. Phys*. **1993**, *176*, 467.

(11) Bixon, M.; Jortner, J. *Adv. Chem. Phys.* **1999**, *106*, 35.

(12) Mataga, N.; Miyasaka, H. *Adv. Chem. Phys.* **1999**, *107*, 431.

(13) Matsuda, N.; Kakitani, T.; Denda, T.; Mataga, N. *Chem. Phys*. **1995**, *190*, 83.

(14) Rehm, D.; Weller, A. *Isr. J. Chem.* **1970**, *8*, 259.

(15) Asahi, T.; Ohkohchi, M.; Matsusaka, R.; Mataga, N.; Zhang, R. P.; Osuka, A.; Maruyama, K. *J. Am. Chem. Soc.* **1993**, *115*, 5665.

(16) (a) Häberle, T.; Hirsch, J.; Pöllinger, F.; Heitele, H.; Michel-Beyerle, M. E.; Anders, C.; Döhling, A.; Krieger, C.; Rückemann, A.; Staab, H. A. *J. Phys. Chem.* **1996**, *100*, 18269. (b) Pöllinger, F.; Musewald, C.; Heitele, H.; Michel-Beyerle, M. E.; Anders, C.; Futcher, M.; Voit, G.; Staab, H. A. *Ber. Bunsen-Ges. Phys. Chem.* **1996**, *100*, 2076.

(17) Wynne, K.; Le Cours, S. M.; Galli, C.; Therien, M. J.; Hochstrasser, R. M. *J. Am. Chem. Soc.* **1995**, *117*, 3749.

(18) (a) Dalton, J.; Milgrom, L. R. *J. Chem. Soc., Chem. Commun.* **1979**, 609. (b) Harriman, A.; Hosie, R. J. *J. Photochem.* **1981**, *15*, 163. (c) Bergkamp, M. A.; Dalton, J.; Netzel, T. L. *J. Am. Chem. Soc.* **1982**, *104*, 253.

(19) (a) Osuka, A.; Mataga, N.; Okada, T. *Pure Appl. Chem.* **1997**, *69*, 797. (b) Osuka, A.; Noya, G.; Taniguchi, S.; Okada, T.; Nishimura, Y.; Yamazaki, I.; Mataga, N. *Chem.—Eur. J*. **2000**, *6*, 33.

(20) Åkesson, E.; Johnson, A. E.; Levinger, N. E.; Walker, G. C.; DuBruil, T. P.; Barbara, P. F. *J. Chem. Phys.* **1992**, *96*, 7859.

(21) Walker, G. C.; Åkesson, E.; Johnson, A. E.; Levinger, N. E.; Walker, G. C.; Barbara, P. F. *J. Chem. Phys.* **1992**, *96*, 3728.

(22) Bixon, M.; Jortner, J.; Cortes, J.; Heitele, H.; Michel-Beyerle, M. E. *J. Phys. Chem.* **1994**, *98*, 7289.

(23) Islampour, R.; Alden, R. G.; Wu, G. Y. C.; Lin, S. H. *J. Phys. Chem.* **1993**, *97*, 6793.

(24) Reid, P. J.; Barbara, P. F. *J. Phys. Chem.* **1995**, *99*, 3554.

(25) Rosenthal, S. J.; Xie, X.; Du, M.; Fleming, G. R. *J. Chem. Phys.* **1991**, *95*, 4715.

(26) Jimenez, R.; Fleming, G. R.; Kumar, P. V.; Maroncelli, M. *Nature (London)* **1994**, *369*, 471.

(27) Fainberg, D. B.; Huppert, D. *Adv. Chem. Phys.* **1999**, *107*, 191.

(28) Bagchi, B.; Gayathri, N. *Adv. Chem. Phys.* **1999**, *107*, 1.

(29) Raineri, F. O.; Resat, H.; Perng, B.-C.; Hirata, F.; Friedman, H. L. *J. Chem. Phys.* **1994**, *100*, 1477.

(30) Mataga, N. *Pure Appl. Chem.* **1997**, *69*, 729.

(31) Mataga, N. In *The Exciplex;* Gordon, M., Ware W. R., Eds.; Academic Press: New York, 1975; p 113.

(32) Hirata, Y.; Kanda, Y.; Mataga, N. *J. Phys. Chem.* **1983**, *87*, 1657.

(33) Asahi, T.; Ohkohchi, M.; Mataga, N. *J. Phys. Chem*. **1993**, *97*, 13132.

(34) (a) Miyasaka, H.; Tabata, A.; Kamada, K.; Mataga, N. *J. Am. Chem. Soc*. **1993**, *115*, 7335. (b) Miyasaka, H.; Tabata, A.; Ojima, S.; Ikeda, N.; Mataga, N. *J. Phys. Chem.* **1993**, *97*, 8222.

(35) Miyasaka, H.; Kotani, S.; Itaya, A.; Schweitzer, G.; DeSchryver, F.; Mataga, N. *J. Phys. Chem. B* **1997**, *101*, 7978.

(36) Englman, R.; Jortner, J. *Mol. Phys*. **1970**, *18*, 145.

(37) Kubo, R.; Toyozawa, Y. *Prog. Theor. Phys*. **1955**, *13*, 160.

(38) Mataga, N.; Shibata, Y.; Chosrowjan, H.; Yoshida, N.; Osuka, A. *J. Phys. Chem. B* **2000**, *104*, 4001.

(39) Yoshida, N.; Ishizuka, T.; Osuka, A.; Okada, T.; Miyasaka, H.; Murakami, M.; Itaya, A.; Nagata, Y. To be submitted for publication.

(40) Hirata, Y.; Mashima, K.; Fukumoto, H.; Tani, K.; Okada T. *Chem. Phys. Lett*. **1999**, *308*, 176.

(41) (a) Ulstrup, J.; Jortner, J. *J. Chem. Phys*. **1975**, *63*, 4358. (b) Jortner, J. *J. Chem. Phys*. **1976**, *64*, 4860.

(42) (a) Perng, B.-C.; Newton, M. D.; Raineri, F. O.; Friedman, H. L. *J. Chem. Phys.* **1996**, *104*, 7153. (b) Perng, B.-C.; Newton, M. D.; Raineri, F. O.; Friedman, H. L. *J. Chem. Phys.* **1996**, *104*, 7177.

(43) Jeon, J.; Kim, H. J. *J. Phys. Chem. A* **2000**, *104*, 9812.

(44) (a) Mataga, N.; Kaifu, Y.; Koizumi, M. *Bull. Chem. Soc. Jpn*. **1955**, *28*, 690. (b) Mataga, N.; Kaifu, Y.; Koizumi, M. *Bull. Chem. Soc. Jpn.* **1956**, *29*, 465.

(45) (a) Lippert, E. *Z. Naturforsch.* **1955**, *109*, 541. (b) Lippert, E. *Ber. Bunsen-Ges. Phys. Chem.* **1957**, *61*, 962.

(46) Ras, A. M.; Bordewijk, P. *Recl. Trav. Chim. Pays-Bas* **1971**, *90*, 1055.

(47) Reichard, C. *Solvents and Solvent Effects in Organic Chemistry*; VCH-Verlag: Weinheim, Germany, 1990.

(48) Wynne, K.; Galli, C.; Hochstrasser, R. M. *J. Chem. Phys*. **1994**, *100*, 4797.

(49) Horng, M. L.; Gardecki, J.; Papazyan, A.; Maroncelli, M. *J. Phys. Chem*. **1995**, *99*, 17311.

(50) Sumi, H.; Marcus, R. A. *J. Chem. Phys.* **1986**, *84*, 4894.

(51) (a) Viehbeck, A.; Goldberg, M. J.; Lavoc, C. A. *J. Electrochem. Soc.* **1990**, *137*, 1460. (b) Rak, S. F.; Jozefiak, T. H.; Miller, L. L. *J. Org. Chem.* **1990**, *55*, 4794.

(52) Chang, Y. J.; Castner, E. W., Jr. *J. Chem. Phys.* **1993**, *99*, 7289.